isvr Institute of Sound and Vibration Research

Gradient Projection Methods for Boundary Layer Transition Control

O.R. Tutty, P. Hackenberg and P.A. Nelson

ISVR Technical Report No. 284

August 1999

University of Southampton

SCIENTIFIC PUBLICATIONS BY THE ISVR

Technical Reports are published to promote timely dissemination of research results by ISVR personnel. This medium permits more detailed presentation than is usually acceptable for scientific journals. Responsibility for both the content and any opinions expressed rests entirely with the author(s).

Technical Memoranda are produced to enable the early or preliminary release of information by ISVR personnel where such release is deemed to the appropriate. Information contained in these memoranda may be incomplete, or form part of a continuing programme; this should be borne in mind when using or quoting from these documents.

Contract Reports are produced to record the results of scientific work carried out for sponsors, under contract. The ISVR treats these reports as confidential to sponsors and does not make them available for general circulation. Individual sponsors may, however, authorize subsequent release of the material.

UNIVERSITY OF SOUTHAMPTON

INSTITUTE OF SOUND AND VIBRATION RESEARCH

FLUID DYNAMICS AND ACOUSTICS GROUP

Gradient Projection Methods for Boundary Layer Transition Control

by

O R Tutty, P Hackenberg and P A Nelson

ISVR Technical Report No. 284

August 1999

Authorized for issue by
Professor P A Nelson
Group Chairman

CONTENTS

FIGURES

Figure 1. The suction coefficient C_qx10^4 versus x_T for a single suction panel at $0.4 \leq x \leq 0.72$

Figure 2. Transition position for two suction panels as a function of the C_qx10^4. The contours are for constant x_T up to $x_T = 1.5$ in increments of 0.1. Also shown is the contour for the optimum value of the cost function when $x_d = 1.5$. The optimum is given by the point closest to the origin where the lines are tangential.

Figure 3. Transition position x_T and suction flow rates (C_qx10^4) against iteration number k for two panel flat plate case. Solid line, panel one, dashed line, panel two.

Figure 4. Cost function ($10^8 \sum C_q^2$) against iteration number k for two panel flat plate case. Solid line, $\gamma_0 = 1.0$, dashed line $\gamma_0 = 0.5$, dotted line $\gamma = 0.25$.

Figure 5. Suction distributions (C_qx10^4) for the six panel flat plate case. The transition positions are $x_T = 1.7$, 2.0, 2.3, 2.6 and 2.9 for the solid line to the dot-dash line respectively.

Figure 6. The cost ($10^8 \sum C_q^2$) against transition position for the suction distributions shown in figure 5.

Figure 7. The transition position, cost ($10^8 \sum C_q^2$), and suction flow rate (C_qx10^4) for panel four for the six panel flat plate case, for $x_d = 2.0$ (solid line), 2.3 (long dashes), and 2.6 (short dashes).

Figure 8. The pressure distribution for inviscid flow past the hump.

Figure 9. Transition position x_T against iteration number k for six panels with a pressure gradient.

Figure 10. Transition position for two suction panels as a function of the C_qx10^4. The contours are for constant x_T from 1.3 to 2.4 in increments of 0.1 omitting 1.6. Also shown are a number of contours of constant cost.

Figure 11. Transition position x_T against the suction flow rate on panel 1 (C_qx10^4) with $C_q = 2\text{x}10^{-4}$ on panel 2.

Figure 12. Amplification factor $N(x)$ for a flat plate with nosuction (solid line), a hump with no suction (short dashes), and a hump with two panels and $C_{q1} = 4\text{x}10^{-5}$ and $C_{q2} = 2\text{x}10^{-4}$ (dots), and $C_{q1} = 5\text{x}10^{-5}$ and $C_{q2} = 2\text{x}10^{-4}$ (dot-dash). These lines have predicted transition position of $x_T = 0.92$, 1.20, 1.40 and 1.89 in turn. The dashed line shows the critical value of $n = 4.3$.

ABSTRACT

In recent years there has been increasing interest in the control of boundary-layer transition through the use of surface suction. Here the use is considered of multiple suction panels to delay transition for cases with or without a pressure gradient imposed by the external inviscid flow. The aim is to maintain transition at a desired location with minimum cost, defined as the sum of squares of the individual suction flow rates, through an automatic adaptive feedback control loop which regulates the suction flow rates by solving a constrained optimisation problem. Numerically, two-dimensional boundary layer flow was calculated using an interactive formulation, and linear stability theory was used to calculate the spatial growth rates of Tollmien-Schlichting waves, with the location of transition predicted via the e^N-method. The optimisation strategy was then used to update the suction flow rates. It was found that when the problem is well specified, i.e. an appropriate transition position is used, the method quickly converges. However, for at least one case it was found that there was no single optimum solution within the numerical tolerance of the method. Further, for a different problem, there are regions between the maximum and minimum transition position which are not accessible, and other positions for which a solution exists but to which the solution algorithm cannot converge as they occur at a discontinuity in the relationship between the transition position and the suction flow rates. Such difficulties could also occur in other suction optimisation formulations, and when using different solution algorithms.

1. Introduction

The possibility of controlling boundary layers to delay transition is a subject that has received much attention within the aerodynamics research community (see the review by Gad-el-Hak [1]) because of the lower skin friction drag in laminar flow. It has long been known that small amounts of surface suction can, in theory, greatly enhance the stability characteristics of an attached boundary-layer, and thereby reduce drag and hence operating costs by delaying transition. A number of attempts have been made in the past to employ such technology, which have been thoroughly reviewed by Joslin [2]. Recently there has been a resurgence of interest in suction as a control mechanism, prompted largely by the development of such technology as low cost, laser drilled, titanium sheets which, when utilised as suction panels, avoid many of the mechanical problems which bedeviled earlier attempts to use suction in practice.

Suction stabilises the boundary layer by inhibiting its growth, and changing the curvature of the velocity profile so that the stability characteristics of the flow are improved. For efficient application of this technique in practice, multiple suction panels with independent suction flow rates are required. These suction flow rates should be monitored constantly due to the possible changes of flow parameters during operation. This clearly indicates the need for an automatic, adaptive, computer based control system, which will allow a continuous modification of the boundary layer flow by adjusting the individual suction flow rates to maintain transition at a desired location with minimum effort.

At Southampton over the past eight years there has been a programme of research into the experimental application of distributed suction for the automatic control of boundary layer transition. In the initial work a plate with two independent suction panels was used, either with or without a free stream pressure gradient. In the initial experiments [3] it was shown that transition can be detected by means of surface pressure fluctuations, and that using these pressure measurements, transition can be maintained at a fixed location using a single input/single output feedback control system. In subsequent experiments with two suction panels [4], the individual suction flow rates were controlled maintaining transition at a desired location while minimising a cost function based on the sum of squares of the suction flow rates. This cost function was chosen as it gives a rough approximation to the power consumption of the pumps of used in the suction system. The combination of the minimisation of the cost function with a fixed transition position gives a non-linearly constrained optimisation problem. To solve this problem, an algorithm was developed [5] using the ideas behind the modified least mean-squares algorithm of Frost [6] which is based on the gradient projection method. More recently the plate rig has been extended to handle four independent suction panels [7], while development work is proceeding on a two metre chord aerofoil with four suction panels which will be installed in a large, low turbulence wind tunnel.

In addition to the experimental work, which is detailed in [3, 4, 5], a complementary

programme of theoretical modelling has been performed. This work was aimed at both modelling the experiments and extending the scope of the research by considering more suction panels and more realistic geometries such as NACA aerofoils. It is of course a much simpler task to change the specification of the problem through computational modelling than changing an experimental rig, provided it has been demonstrated that the modelling can satisfactorily reproduce the behaviour of the experiments. The modelling consists of an interactive boundary layer formulation for the flow, a stability analysis using linear stability theory, transition prediction using the e^N method, followed by an update of the suction flow rates using the same basic strategy as used in the experiments. This paper presents the major results from the theoretical modelling. In addition to the results presented below, which are largely new, details of our early work in this area which can be found in [8]. A brief overview of both the initial experimental and theoretical work can be found in [9].

2. Problem Formulation

For the basic flow standard dimensionless boundary layer coordinates and velocities are adopted as follows

$$u = \frac{\tilde{u}}{\tilde{U}_\infty}, \quad v = \frac{\tilde{v}}{\tilde{U}_\infty}\sqrt{R}, \quad x = \frac{\tilde{x}}{\tilde{L}}, \quad y = \frac{\tilde{y}}{\tilde{L}}\sqrt{R} \tag{1}$$

where u and v are the streamwise and the transverse velocities in the x and y directions respectively, "~" denotes dimensional values, $\tilde{U}_\infty$ the free-stream velocity, $\tilde{L}$ is the characteristic length in the direction of the flow, and R is the Reynolds number based on $\tilde{U}_\infty$ and $\tilde{L}$. The boundary layer equations then become

$$u\frac{\partial u}{\partial x} + v\frac{\partial u}{\partial y} = u_e\frac{du_e}{dx} + \frac{\partial^2 u}{\partial y^2} \tag{2}$$

$$\frac{\partial u}{\partial x} + \frac{\partial v}{\partial y} = 0 \tag{3}$$

with boundary and initial conditions

$$y = 0: \quad u = 0\,, \quad v = v_w \tag{4}$$

$$y \to \infty: \quad u(x,y) \to u_e(x) \tag{5}$$

$$u_e(x) = u_{e_0}(x) + \frac{1}{\pi\sqrt{R}}\int_{x_0}^{x_1} \frac{\frac{\partial(u_e\delta^*)}{\partial\xi}}{x-\xi}d\xi \tag{6}$$

$$x = x_0: \quad \text{Blasius profile} \tag{7}$$

where u_e is the external velocity at the outer edge of the boundary layer, δ^* is the dimensionless displacement thickness, and v_w is the imposed surface suction velocity distribution, which, assuming discrete suction panels, is piecewise constant. The first part of the edge velocity, u_{e_0}, comes from the standard potential solution for inviscid flow past the surface, and the second part is a correction due to the displacement of the streamlines which allows an interaction between the inviscid and viscous parts

of the flow field over the range $[x_0, x_1]$, following Carter and Wornom [10]. The effect of the interaction of the boundary layer with the outer inviscid flow is most pronounced at the ends of the suction panels where the boundary condition at the wall is discontinuous, and the solution with interaction is much smoother than that without interaction.

In this work it is assumed that the transition from laminar to turbulent flow is initiated by the amplification of small two-dimensional travelling Tollmien-Schlichting waves rather than through a bypass mechanism. Hence spatial linear stability theory is used, with the disturbance to the flow given by a normal mode of the form

$$\phi(x, y, t) = \Phi(y) e^{i(\alpha x - \omega t)} \tag{8}$$

where ϕ is the dimensionless disturbance streamfunction, α is the complex wave number, ω is the real frequency of the disturbance and Φ its amplitude. Substitution into the Navier-Stokes equations and linearisation now produces the governing equation for Φ.

$$\left(u - \frac{\omega}{\alpha}\right)\left(\Phi'' - \alpha^2\Phi\right) - u''\Phi - \frac{i}{\alpha}\left[v\left(\Phi''' - \alpha^2\Phi'\right) - \frac{1}{Re}\left(\Phi'''' - 2\alpha^2\Phi'' + \alpha^4\Phi\right)\right] = 0. \tag{9}$$

Here u and v are the velocity components of the mean flow obtained from (2-7), Re is the Reynolds number based on the local boundary layer thickness, and the prime denotes differentiation with respect to y. Note that there is an implicit rescaling here between the variables used for the flow calculation and the stability calculation.

Equation (9) presents an eigenvalue problem with homogeneous boundary conditions since the disturbance velocities must vanish at the wall and in the free stream. It resembles the usual Orr-Sommerfeld equation with an additional term involving the vertical mean-flow velocity which arises from the effect of wall suction. This extra term is included as it will be at least the order of magnitude of the viscous terms: the well known asymptotic suction profile with constant suction on a flat plate has $v = O(Re^{-1})$, and since the critical suction rate for unconditional (linear) stability of this asymptotic profile is known to be too small in practice, we expect that our suctions rates will be at least of $O(Re^{-1})$. For a given Reynolds number and real frequency the solution yields an eigenfunction in form of the complex disturbance amplitude and the complex wave number as the eigenvalue. The imaginary part of the wave number is the spatial growth rate which is positive for damped waves and negative for amplified waves.

Once the eigenvalues have been obtained, the empirical e^N method developed by Smith [11] and Van Ingen [12] is used to predict the position of transition. The e^N method relates the point of transition to the amplification of the disturbance modes. For a fixed frequency ω, the amplification factor is integrated to obtain the N value for that frequency,

$$N_\omega(x) = \ln\left(\frac{A}{A_N}\right) = -\int_{x_N}^{x} \alpha_i dx \tag{10}$$

A is the amplitude of the wave and the subscript N refers to the neutral point where $\alpha_i = 0$. The standard e^N is based on the envelope of the amplification curves, where N is given by the maximum amplification factor at each point,

$$N(x) = max_\omega \left[N_w\right]. \tag{11}$$

The transition point, x_T, is then predicted to be the first point at which N exceeds the critical value N_T at which transition will occur. In any particular situation the appropriate value of N_T depends on the background turbulence. For low free-stream turbulence levels, typically values of eight to 10 will be used for N_T. However, Mack [13] has shown that N_T is strongly dependent on the turbulence level, and suggest the following relation

$$N_T = -8.43 - 2.4 \ln_e Tu \tag{12}$$

where the turbulence level is calculated as

$$Tu = \sqrt{\frac{\overline{u'^2} + \overline{v'^2} + \overline{w'^2}}{3}}, \tag{13}$$

with (u', v', w') the dimensionless disturbance velocities in the usual form. For the initial experiments with the plate rig value of N_T is determined by comparisons with the experiments of Nelson et.al. [14]. Calculating the envelope curve for the boundary-layer flow without suction yields $N_T = 4.3$ since the free-stream turbulence level in the wind tunnel used for these experiments is approximately 1%.

Given the prediction of the transition point, we now wish to adjust the suction rates following the same procedure used in the experiments, i.e. maintain transition at a desired location while minimising the sum of squares of the suction flow rates. The constrained optimisation problem can be stated as

$$\text{minimize} \qquad \phi(\underline{u}) = \underline{u}^T \underline{u} \tag{14}$$

$$\text{subject to} \qquad e(\underline{u}) = x_T - x_d = 0 \tag{15}$$

where $\underline{u}$ is the vector of suction flow rates and x_d is the desired transition position. Note that this formulation assumes that the suction rate is constant on each panel and implicitly that all panels have the same length since all suction flow rates are given the same weight. A solution algorithm for (14,15) can be obtained using a steepest descent technique [4, 5], where the update of the suction flow rates from iteration k to $k+1$ is given by

$$\underline{u}_{k+1} = \underline{u}_k - \mu \mathbf{D}_k \underline{u}_k - (1-\alpha)\underline{\theta}_k \left[\underline{\theta}_k^T \underline{\theta}_k\right]^{-1} e_k \tag{16}$$

where

$$\mathbf{D}_k = \mathbf{I} - \underline{\theta}_k \left[\underline{\theta}_k^T \underline{\theta}_k\right]^{-1} \underline{\theta}_k^T \tag{17}$$

Here μ is the gain, it is assumed that the error is reduced by a constant factor each iteration so that

$$e_{k+1} = \alpha e_k \tag{18}$$

and $\underline{\theta}_k = \nabla e_k$ is the gradient of the "error" with respect to the suction flow rates.

The algorithm requires an estimate of $\underline{\theta}_k$ at each iteration. One way of doing this is to use a finite difference approach, i.e. add and subtract a small increment to each of the current suction rates in turn, estimate the transition position for each of these new flow rates, and use the changes in x_T to estimate $\underline{\theta}_k$. There are a number of disadvantages to this approach. An obvious one is that the number of function evaluations (flow, stability and transition calculations) increases with the number of suction panels, leading to a large increase in the computational effort each time the suction flow rates are updated. Further, in a noisy experimental situation such a procedure may not be well conditioned. Accordingly, an alternative approach, based on that used in the initial experiments [9], will be investigated. A local linear model of the dependence of the change of transition position on the change in the suction flow rates is assumed, and this model is updated as the iterations proceed. Specifically, a small change $\delta\underline{u}$ in the vector of suction flow rates will give a change in the transition position δx_T, which is written as

$$\delta x_T = \delta \underline{u}^T \underline{\theta}_k + n \tag{19}$$

where n is the error. Note that in general n will be nonzero since the relationship between x_T and $\underline{u}$ is nonlinear. Applying this relationship over the previous K iterations gives

$$\begin{bmatrix} \delta x_{T(k-K)} \\ \vdots \\ \delta x_{T(k-1)} \\ \delta x_{Tk} \end{bmatrix} = \begin{bmatrix} \delta \underline{u}^T_{(k-K)} \\ \vdots \\ \delta \underline{u}^T_{(k-1)} \\ \delta \underline{u}^T_k \end{bmatrix} \underline{\theta}_k + \begin{bmatrix} n_{(k-K)} \\ \vdots \\ n_{(k-1)} \\ n_k \end{bmatrix} \tag{20}$$

which can be written compactly as

$$\delta \underline{x}_k = \delta \underline{U}_k \underline{\theta}_k + \underline{n}_k \tag{21}$$

An estimate of $\underline{\theta}_k$ could now be obtained using a least squares approach by minimising $\underline{n}_k^T \underline{n}_k$. However this could result in large errors since it places equal weight on the data from each iteration, including previous steps when the gradient may have been very different. Therefore to give less weight to older data, a "forgetting factor" γ is introduced, and $\underline{\theta}_k$ is determined by minimising the cost function

$$J_\gamma = \underline{n}_k^T \mathbf{\Gamma}_k \underline{n}_k \tag{22}$$

where $\mathbf{\Gamma}_k$ is the diagonal matrix given by

$$\mathbf{\Gamma}_k = \text{daig}(\gamma^K, \gamma^{K-1}, ..., \gamma^2, \gamma, 1) \tag{23}$$

The solution is

$$\underline{\theta}_k = [\delta \underline{U}_k^T \mathbf{\Gamma}_k \delta \underline{U}_k]^{-1} \delta \underline{U}_k^T \mathbf{\Gamma}_k \delta \underline{x}_k \tag{24}$$

The explicit inversion of the matrix $\delta \underline{U}_k^T \mathbf{\Gamma}_k \delta \underline{U}_k$ in (24) can be avoided by the use of the Recursive Least Squares algorithm (RLS). Full details can be found, for example, in Wellstead and Zarrop [15]. At each new iteration $\underline{\theta}_{k+1}$ is evaluated from implementing the following:

i. Calculate

$$n_{k+1} = \delta x_{T(k+1)} - \delta \underline{u}_{k+1}^T \underline{\theta}_k \tag{25}$$

ii. Form the matrix $\mathbf{P}_{k+1} = [\delta \underline{U}_{k+1}^T \mathbf{\Gamma}_k \delta \underline{U}_{k+1}]^{-1}$ from the recursion

$$\mathbf{P}_{k+1} = \frac{1}{\gamma} \mathbf{P}_k \left[\mathbf{I} - \frac{\delta \underline{u}_{k+1} \delta \underline{u}_{k+1}^T \mathbf{P}_k}{\gamma + \delta \underline{u}_{k+1}^T \mathbf{P}_k \delta \underline{u}_{k+1}} \right] \tag{26}$$

iii. Update the estimate of the gradient from

$$\underline{\theta}_{k+1} = \underline{\theta}_k + \mathbf{P}_{k+1} \delta \underline{u}_{k+1} n_{k+1} \tag{27}$$

In this form the parameter identification routine needs an initial estimate $\mathbf{P}_0$ of the covariance matrix $\mathbf{P}_k$. A standard choice, the identity matrix scaled by a large positive constant (10^4), was used. The elements of $\underline{\theta}_0$ were set to a negative constant (-50).

The form of the forgetting factor must also be specified. This was adjusted at each iteration so that the information content was kept constant [16] using

$$\gamma = \left(1 - \frac{\sigma_0 n_{k+1}^2}{1 + \delta \underline{u}_{k+1}^T \mathbf{P}_k \delta \underline{u}_{k+1}} \right) \gamma_0 \tag{28}$$

where σ_0 and $\gamma_0 \leq 0$ are positive constants. Also, in the RLS procedure a small random perturbation was to the suction flow rates at each iteration. This is analogous to the "dither" added to the signal when using the RLS algorithm for system identification and helps prevent the phenomenon of "estimator wind-up" [15] which can cause the gradient estimation routine to fail after a large number of iterations.

The accuracy and efficiency of this gradient estimation algorithm will depend on a number of factors, including the size of the of the various parameters, specifically the forgetting factor γ, and the nature of the error surface. It may well be prone to error due to the implicit assumption of validity of past data. However, it has the considerable advantage of operating entirely on known data: each time the suction flow rates are updated and a new transition position is calculated, this provides the necessary changes in variables required to update $\underline{\theta}_{k+1}$ using (25-28). In contrast, at each iteration a finite difference scheme will at least as many perturbations as there are suction panels. Thus, the use of the RLS method has the potential to produce a much more efficient algorithm in terms of the number of function evaluation required to obtain the optimum in the numerical simulations, or equivalently, the number of samples necessary in the experimental case.

To complete the algorithm, the remaining parameters must be specified. In the update of the suction velocities (16), the size of α and μ reflect the weighting given to the term reducing the error and the cost, respectively. In this work $\alpha = 0$, was used throughout, while $\mu = \frac{1}{2}$ was found to give good results in most cases, and unless otherwise mentioned it was used to obtain the results presented below. In the

forgetting factor, γ, $\sigma_0 = \frac{1}{80}$ was used throughout, while $\gamma_0 = \frac{1}{2}$ was used for most of the results presented here. The smaller the value of γ_0, which must lie in the range $0 < \gamma_0 \leq 1$, the less the influence of the older information, and as will be seen below, making γ_0 small enough is crucial to the efficient operation of the entire optimisation procedure.

In system identification problems using the RLS method, a covariance resetting procedure is sometimes employed. The idea here is to prevent premature convergence of the algorithm where the gradient estimate locks onto a set of incorrect values, by resetting the matrix $\mathbf{P}_k$. A procedure of this kind, where the off diagonal elements of $\mathbf{P}_k$ were set to zero and the diagonal elements multiplied by 50, was used here, with the resetting occurring every 50 iterations.

As already noted, the major advantage of the RLS for parameter identification over the conceptually simple finite difference approach, is that when it works it will be much more efficient, particularly with a large number of panels. However, both were investigated, and they will be compared below.

The method presented above searches for the optimum suction distribution by calculating in turn the flow field, the stability characteristics, and the transition position, following by an update in the suction flow rates, with the loop repeated as often as necessary. This could be regarded as a quasi-steady analysis in which the system is allowed to settle down before the transition position is estimated and the suction flow rates are updated. In this it mimics the experimental situation [3], in which it was found necessary to allow a sufficiently long sample time so that the system converged to its new state before the suction flow rates were updated. If the sample time was too short, then the scheme had problems converging onto a solution.

3. Results

Flat plate with one suction panel

As a reference case, take air at standard conditions ($\nu = 1.5\text{x}10^{-5}\text{m}^2\text{s}^{-1}$) with $\tilde{U} = 20\text{ms}^{-1}$, $N_T = 4.3$ and $\tilde{L} = 1\text{m}$. With these values and no suction, transition is predicted to occur at $x \approx 0.92$, where $x = 0$ is the leading edge of the plate. Hence, since the aim is to delay transition through the control of small amplitude disturbance, the suction panel must have at least its leading edge upstream of this position. Figure 1 shows the transition position for different suction flow rates for a suction panel in the region $0.4 \leq x \leq 0.72$, where the suction flow rate is given in terms of the suction coefficient

$$C_q = -\tilde{v}_w/\tilde{U}. \tag{29}$$

Initially, as suction is applied the change in x_T is close to linear, with a relatively small amount of suction moving transition a significant distance downstream. However, as more suction is applied the slope of the curve changes until it appears to asymptote to a constant transition position. At this point, the boundary layer on the suction panel is extremely thin, and while increasing the suction flow rate will change the transverse

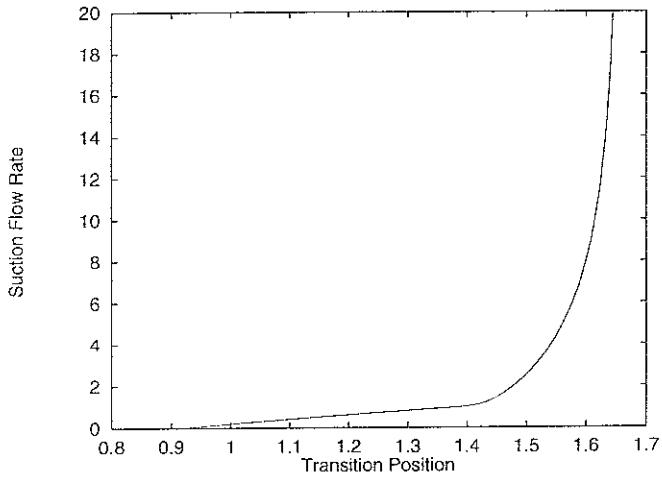

Figure 1: The suction coefficient C_qx10^4 versus x_T for a single suction panel at $0.4 \leq x \leq 0.72$

velocity in the region of the panel, it has little effect on the stability characteristics of the flow downstream of the panel, where the curve of $N_\omega(x)$ shows little variation with v_w. Hence, for a single panel, after a certain point, further suction effort is largely wasted in terms of delaying the onset of transition. Further, once sufficient suction has been applied the amplification factor $N_\omega(x)$ falls below zero at the downstream end of the panel, and the shape of $N_\omega(x)$ is basically the same as that found further upstream when there is no suction. As a result, a good estimate of the maximum distance that transition can be moved downstream is obtained by adding the transition position with zero suction (0.92) to the position of the downstream end of the suction panel ($x_T = 0.92 + 0.72 = 1.64$), as can be seen from figure 1. Note that for all cases tested, the transition position asymptotes to a maximum position downstream at high suction rates, and that for the flat plate, a reasonable estimate of this position is given by adding the natural transition position to the downstream end of the last suction panel, although this estimate is not always as accurate as in this case.

Flat plate with two suction panels

This is a case we wish to investigate in some detail, both because it is the simplest case we can use to investigate the behaviour of the optimisation routine, and because it is one of the main cases investigated experimentally [4]. The suction panels are placed at $0.28 \leq x \leq 0.48$ and $0.58 \leq x \leq 0.78$. Contours of the x_T for combinations of the suction flow rates are shown in figure 2, as is the contour of the cost function for the optimum value when $x_d = 1.5$. In this case, it is clear that there is a single global optimum for each value of x_d, and that for low values of x_d the optimum has essentially the same suction flow rate on both panels. The latter result was found also in the experiments [4].

The full code, including the optimisation routine, was run with zero initial suction and $x_d = 1.5$. The transition position and suction flow rates against the iteration number

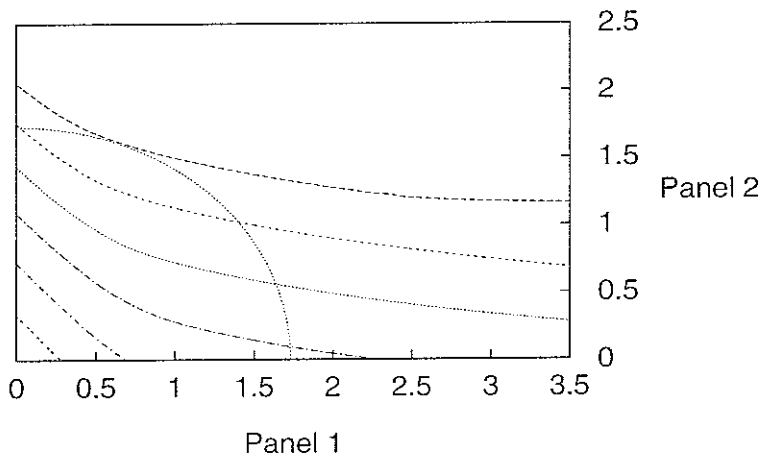

Figure 2: Transition position for two suction panels as a function of the C_qx10^4. The contours are for constant x_T up to $x_T = 1.5$ in increments of 0.1. Also shown is the contour for the optimum value of the cost function when $x_d = 1.5$. The optimum is given by the point closest to the origin where the lines are tangential.

k are shown in figure 3. There is an initial overshoot of the transition position, but this is quickly rectified, with the desired position obtained within 10 iterations and the optimum suction values within 15 iterations. The small scale variation thereafter arises from the dither on the suction flow rates.

In this run, the gradient estimation routine used $\gamma_0 = 0.5$ in (28). Increasing γ_0 to its maximum value of one has a significant effect on the results. The desired transition position is still obtained in 10 iterations, but the optimisation procedure initially settles on a nonoptimum suction distribution with a cost approximately 30% greater than that for the optimum solution, as can be seen from figure 4. The optimum set of flow rates is finally obtained after the second time the matrix $\mathbf{P}_k$ in the gradient estimation routine is reset. The convergence to a set of nonoptimum values indicates a failure of the optimisation procedure as it is clear from figure 2 that there is only a single set of suction values in which the constraint line ($x_d = 1.5$) is tangential to constant cost contour, which is (or should be) the convergence condition for the optimisation procedure. The problem is that with $\gamma_0 = 1.0$ the gradient estimation routine locks too strongly onto the original values and tunes $\underline{\theta}$ to the initial estimate of the slope. This results in the optimisation routine honing in on the set of suction values on the constraint line with almost equal suction values with $C_q \approx 1.5$x10^{-4}.

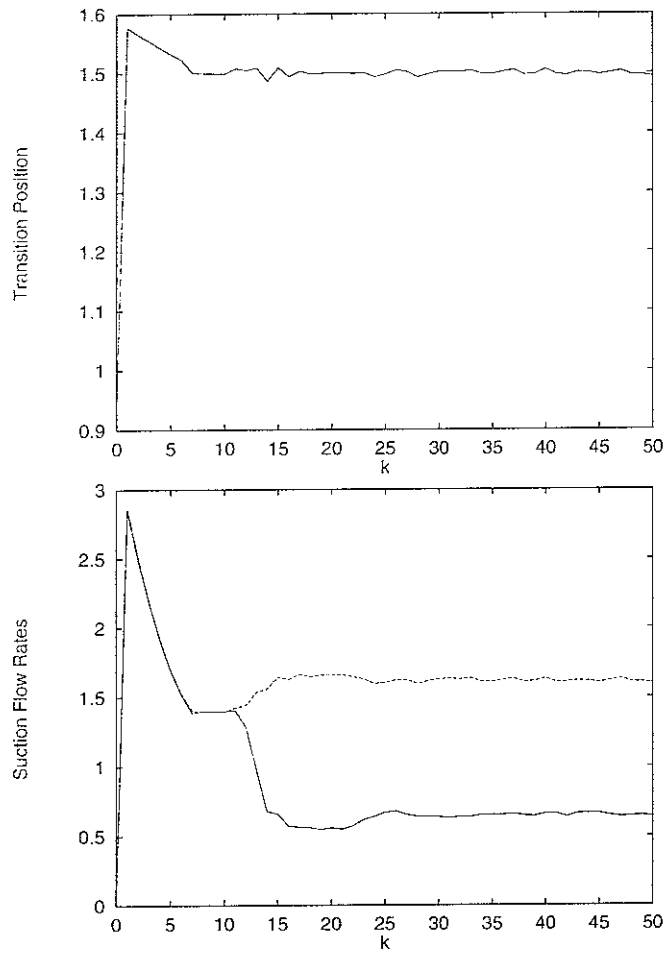

Figure 3: Transition position x_T and suction flow rates (C_qx10^4) against iteration number k for two panel flat plate case. Solid line, panel one, dashed line, panel two.

A large number of test runs have been performed, and premature convergence to a nonoptimum set of values is the standard result when $\gamma_0 = 1.0$, as is a switch to the optimum on the second covariance reset. Clearly γ_0 must be less than one so that less weight is placed on the older values for the algorithm to work properly, and a number of values were tested. With $\gamma_0 = 0.9$ there is still premature convergence, but the switch to the correct solution occurs the first time the covariance is reset. With $\gamma_0 = 0.25$, the optimum is picked up in about the same number of iterations as $\gamma_0 = 0.5$ but there is considerably more variation during the initial stages before the optimum is achieved, but no significant difference thereafter (figure 4).

Flat plate with six suction panels

The experiments have been limited to four suction panels, but the numerical approach employed here can be used to investigate the effect of further panels and different configurations. A large number of runs have been performed, and a representative sample of results can be found in [8]. Here the results for one such case are presented.

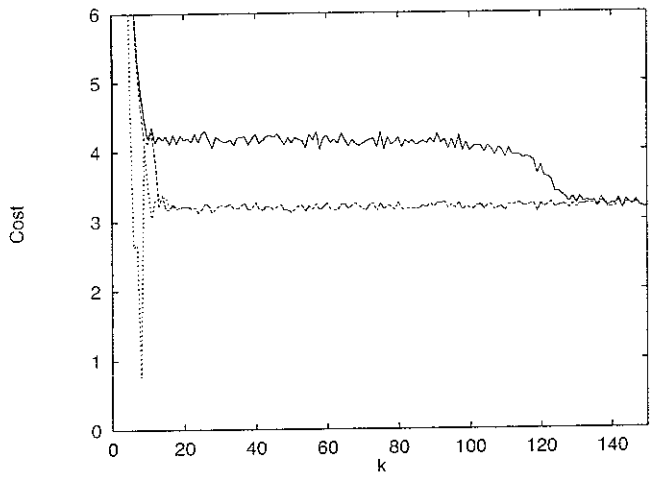

Figure 4: Cost function ($10^8 \sum C_q^2$) against iteration number k for two panel flat plate case. Solid line, $\gamma_0 = 1.0$, dashed line $\gamma_0 = 0.5$. dotted line $\gamma = 0.25$.

Six evenly spaced panels are used. The panels are 0.2 long, with a gap of 0.1 between the panels, and the leading edge of the first panel at $x = 0.3$ and the trailing edge of the final panel at $x = 2.0$. With this configuration and the standard conditions ($\tilde{U}_\infty = 20\text{ms}^{-1}$, $N_T = 4.3$, $\tilde{L} = 1\text{m}$), the maximum distance the transition position can be forced to is $x = 3.0$, slightly more than the distance that would be predicted by adding the natural transition position with no suction to the downstream end of the last suction panel, as was found in the single panel case. Also, since the natural transition position ($x \approx 0.92$) is at the front of the third panel, its is clear that there must be at least some suction on the first two panels, and most probably a spread of the suction effort across a number of the panels.

Suction distributions for six different values of x_d ranging from 1.7 to 2.9 are shown in figure 5. These values have been averaged over a large number of iterations to remove the effects of the dither in the method. In general the first panel($0.3 \leq x \leq 0.5$) makes relatively little contribution to the total suction effort, but as expected the second panel ($0.6 \leq x \leq 0.8$) plays a significant role. The last suction panel ($1.8 \leq x \leq 2$) plays no role when $x_d = 1.7$, as expected as the transition position is now upstream of the leading edge of this panel. It makes some contribution for $x_d \geq 2$, but never has the largest suction even with $x_d = 2.9$. As the transition position moves down the plate the peak suction rate also moves down the plate, from panel two when $x_d = 1.7$ to panel four when $x_d = 2.9$. As expected the cost increases nonlinearly with the increase in x_d, as can be seen from figure 6.

For $x_d = 1.7$, 2.0 and 2.6, the optimum solution is obtained within 25 iterations, and the algorithm holds this solution, except for occasional jumps away when the matrix $\mathbf{P}_k$ in the gradient estimation routine is reset. However, when $x_d = 2.3$ the algorithm is less well behaved, taking around 60 iterations to converge initially, and at times a similar number of iterations to return to the optimum once it has jumped away from

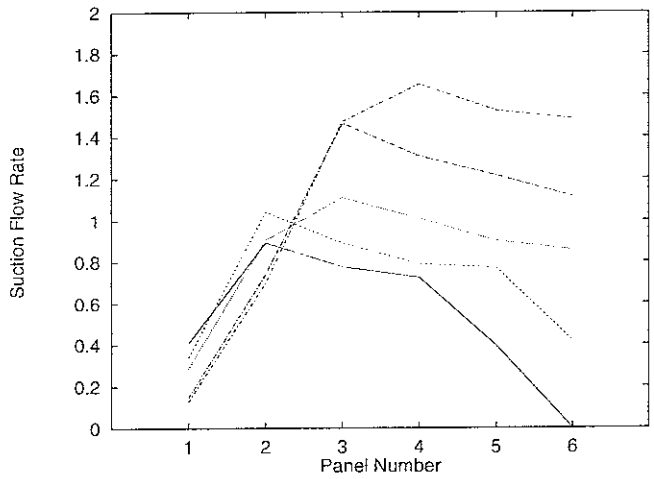

Figure 5: Suction distributions (C_qx10^4) for the six panel flat plate case. The transition positions are x_T = 1.7, 2.0, 2.3, 2.6 and 2.9 for the solid line to the dot-dash line respectively.

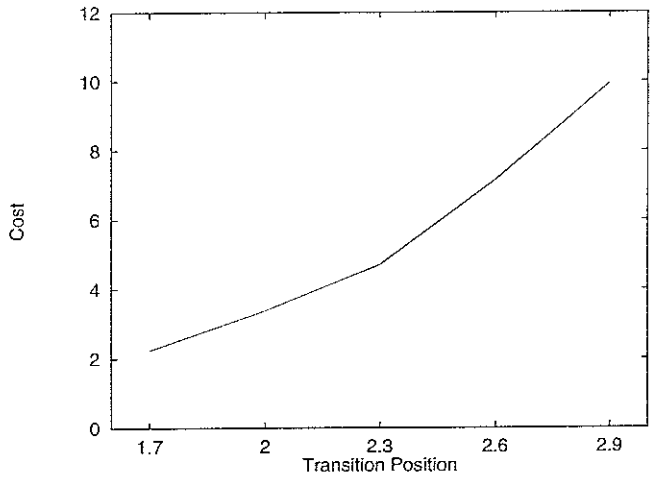

Figure 6: The cost ($10^8 \sum C_q^2$) against transition position for the suction distributions shown in figure 5.

it, e.g. when $\mathbf{P}_k$ is reset. This relatively poor behaviour arises from the fact that the optimisation problem is not well defined for $x_d = 2.3$, at least within the numerical tolerance of the algorithm. Even when the algorithm has locked on to the solution the changes in the individual suction flow rates are at least an order of magnitude greater than those found for $x_d = 2.0$ or 2.6, with variations greater than 10% in the larger flow rates when the predicted value of x_d and the cost are constant to three significant figures. There are also large variations in the components of $\underline{\theta}_k$, and hence problems in regaining an optimum set of values once the optimum has been lost.

For $x_d = 2.9$ it takes around 130 iterations to obtain the best solution, and the algorithm has only limited success in holding to this solution. In a run of 500 iter-

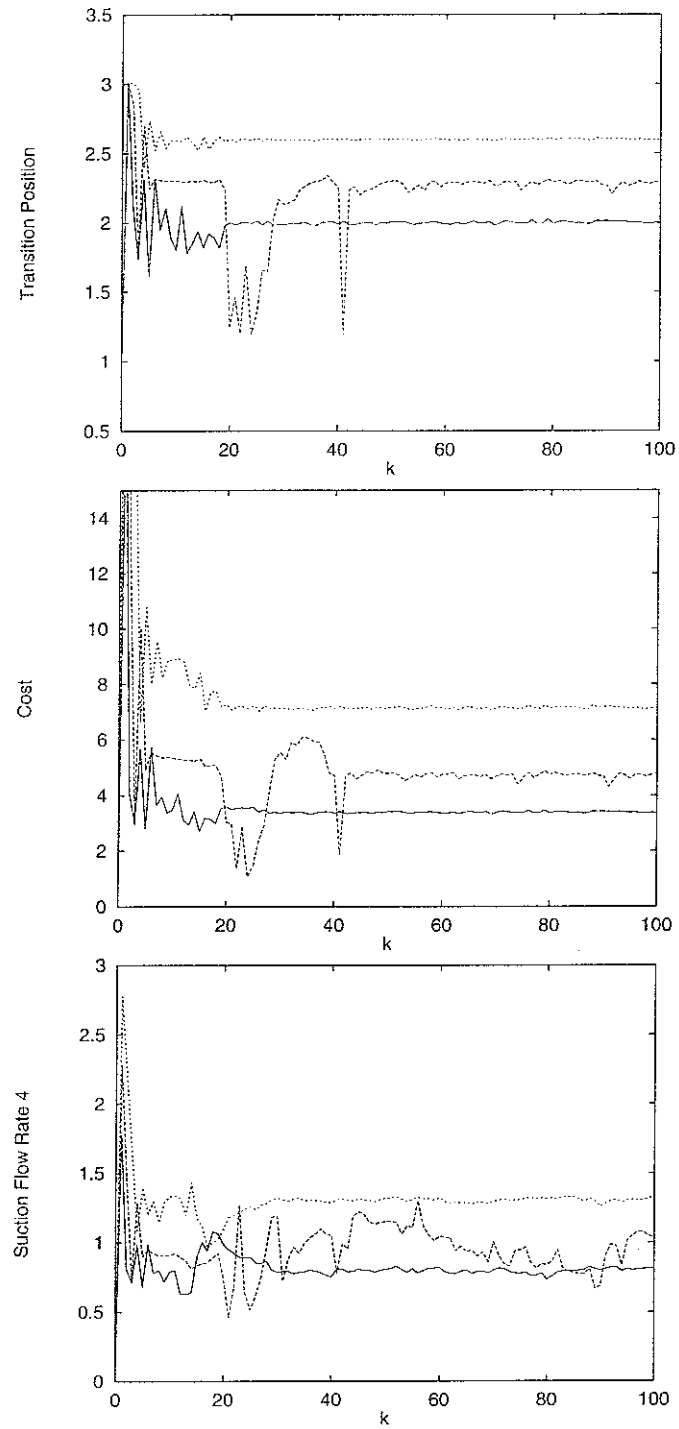

Figure 7: The transition position, cost ($10^8 \sum C_q^2$), and suction flow rate (C_qx10^4) for panel four for the six panel flat plate case, for $x_d = 2.0$ (solid line), 2.3 (long dashes), and 2.6 (short dashes).

ations. the longest the optimum was maintained was around 40 iterations, and once the optimum was lost, the algorithm had difficulty finding it again. Thus, although

an optimum was found, the algorithm could not be said to particularly successful in holding the suction values on this solution. Again there are large variations in the individual flow rates when there is effectively no change in the cost or predicted transition position, which in this case is not surprising given that large changes in the suction flow rates are needed to move the transition position by a significant amount when close to the maximum transition point (see figure 1).

Fine tuning the algorithm can improve the performance in this case. For example, if $\mathbf{P}_k$ is not reset, then once the optimum was found, it was maintained for up to 150 iterations, although there were still jumps away from the optimum and difficulties returning to it. Alternatively, a standard practice in control theory is to allow the gain μ to decay as k increases so that once a solution is obtained, the algorithm will maintain it. A number of different ways of decreasing μ were tried. With $\mu = \mu_0$ for $k \leq 10$ and $\mu = \mu_0/(k-10)$ for $k > 10$, $\mu_0 = 0.5$, the transition position converged to and held the desired value with $x_T = 2.9 \pm 0.01$ within 30 iterations, but took around 500 iterations to obtain the minimum cost of $\sum C_q^2 \approx 10\text{x}10^{-8}$, although it was only 5% above for $k > 100$. Changing μ_0 to 0.25 gave a much slower decay in the cost, with $\sum C_q^2 \approx 10.8\text{x}10^{-8}$ at 500 iterations, although still showing a slow, irregular decay. Generally, it appears that μ must be sufficiently large initially and decay sufficiently slowly that the algorithm can find the optimum before μ becomes too small, and the rate of approach to the optimum becomes too slow. With $\mu = 0.5$ for $k \leq 10$ and $\mu = 2/(k-6)$ for $k > 10$, the desired transition position was obtained with 30 iterations, and the optimum cost with 50 iterations. For the last form of μ, the calculation was repeated with $x_d = 2.3$. This time the optimum solution was obtained efficiently, and was maintained with $x_T = 2.3 \pm .01$ until the run terminated with at $k = 500$, except the first time the matrix $\mathbf{P}_k$ was reset at $k = 50$, when there was a relatively small, short lived, jump away from the optimum. However, there are still relatively large fluctuations in the suction flow rates and components of $\underline{\theta}_k$. Note here, that in all cases the desired transition position was found relatively quickly with $\alpha = 0$, and that it appears that the form of μ is the key element in obtaining and maintaining the optimum.

Plate with a pressure gradient

Although the flat plate configuration provides a convenient test problem, for many applications the pressure gradient from inviscid flow will be nonzero. Experimentally a nonzero pressure gradient was generated by placing a constriction in the tunnel on the wall opposite the flat plate. Numerically, this can be mimicked by calculating the inviscid flow past a wall with a hump using potential theory, and using the velocity at the wall as $u_{e_0}(x)$ in (6). The hump used is

$$y(x) = h.f(z) \tag{30}$$

with

$$f(z) = \begin{cases} 1 - 3z^2 + 2|z|^3 & if\ |z| \leq 1 \\ 0 & if\ |z| < 1 \end{cases} \tag{31}$$

and

$$z = 2(x - x_h)/w_0 \tag{32}$$

where $h = 0.005$, $w_0 = 1$ and $x_h = 1$. The inviscid pressure distribution for this hump is shown in terms of the pressure coefficient $C_p = (p - p_\infty)/\frac{1}{2}\rho U_\infty^2$ in figure 8. There are regions of both favourable and adverse pressure gradient, which, respectively, either locally stabilises or destabilises the flow.

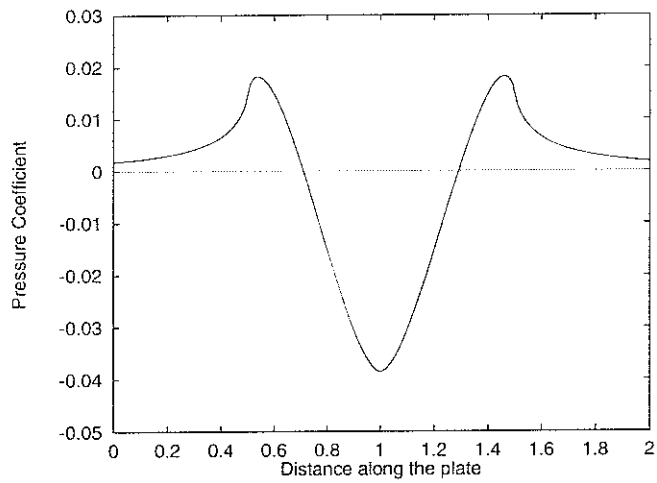

Figure 8: The pressure distribution for inviscid flow past the hump.

A number of runs were performed with this hump and the same six panel configuration used above. For this case the natural transition position with zero suction is at $x \approx 1.12$, and the maximum downstream position of transition is $x \approx 3.05$. With $x_d = 2.6$ the solution was obtained within 30 iterations, and the algorithm had no difficulty maintaining this solution. Not surprisingly, the cost was greater in this case than with the flat plate, with $\sum C_q^2 \approx 1.4\text{x}10^{-7}$, approximately double that with no hump.

Although a solution was obtained for $x_d = 2.6$, for many other values of x_d the algorithm completely failed to converge to or hold on to the desired transition position and associated cost once it had found them. Calculations were performed for $x_d = 1.3$ to 2.7 increasing in steps of 0.1. For $x_d = 1.3$ and 1.4 there was no difficulty in finding a solution. Likewise for $x_d = 2.7$. However for all x_d between 1.5 and 2.5 the algorithm failed to converge. The best behaved of these was with $x_d = 2.5$, as shown in figure 9. Here, although a solution is found with $x_T = 2.5$ on occasions, it is not maintained. Also, the jumps away from the solution do not coincide with the resetting $\mathbf{P}_k$. In all the cases in which the algorithm did not converge the behaviour was worse than that shown in figure 9, i.e. either it could not lock on to a valid solution at all, or was worse at holding on to the solution.

The reasons for this behaviour are best examined using a simpler, two panel, case in which the solution surface can be completely mapped. Consider the case with the

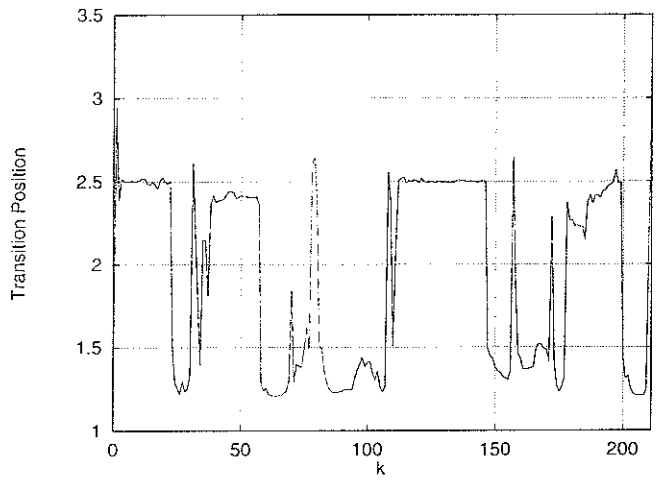

Figure 9: Transition position x_T against iteration number k for six panels with a pressure gradient.

panels at $0.56 \leq x \leq 0.92$ and $1.12 \leq x \leq 1.48$, so that there is one on the upstream and one on the downstream side of the hump. Contours of the transition position versus the suction flow rates plus some of contours of constant cost are shown in figure 10. It can be seen that x_T as a function of the suction flow rates is discontinuous, with the contours of x_T for $x_T \approx 1.5$ to $x_T \approx 2.1$ terminating/originating at the discontinuity on the left of figure 10. This can be seen also in figure 11, which shows the large jump in x_T at the discontinuity as the suction flow rate on panel one changes with a fixed suction rate on panel two. Further, for much of, although not all, of x_T in the range of 1.5 to 2.0, the minimum cost is at the discontinuity. As can be seen from figure 10, for $x_T = 2.0$, although the transition contour terminates at the discontinuity, the minimum cost occurs somewhat to the right of the discontinuity, and numerically the algorithm has no trouble finding the optimum. In fact, the optimum solution is easily obtained for $x_d \leq 1.4$ or $x_d \geq 2.0$, but for x_d between 1.5 and 1.9 the minimum cost is at the discontinuity and the algorithm fails in these cases. Note that allowing the gain μ to decrease as k increases, as in the six panel flat plate case above, does improve the behaviour of the algorithm for x_d between 1.5 and 1.9.

The reason for the discontinuity on the left of figure 10 can be seen from figure 12 which shows the amplification factor $N(x)$ for a number of different configurations. As expected, when there is no suction, in regions of favourable and adverse pressure gradient, as shown in figure 8, the flow is stabilised or destabilised, respectively, resulting in several local extrema in $N(x)$. Applying suction enhances the stability of the boundary layer, and this combined with the underlying stability characteristics of the flow creates a situation where a small increase in the suction can cause the predicted transition position to jump from a point near a local maximum of $N(x)$ to a point much further downstream, again as shown in figure 12. In figure 12 the jump in the transition position was generated by changing the flow rate on the first

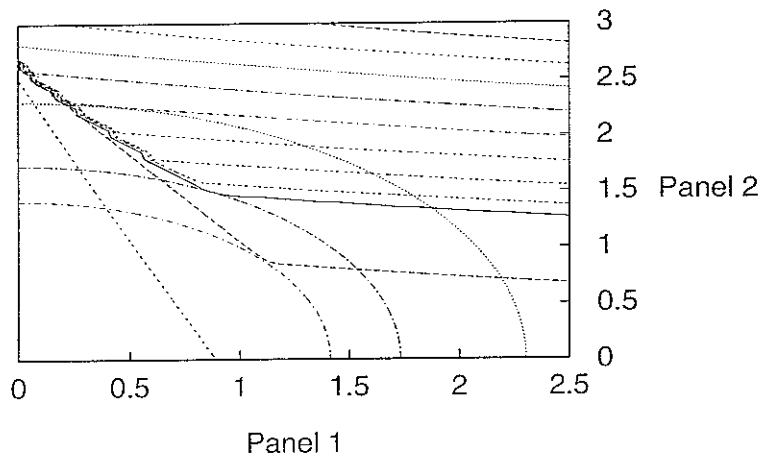

Figure 10: Transition position for two suction panels as a function of the C_qx10^4. The contours are for constant x_T from 1.3 to 2.4 in increments of 0.1 omitting 1.6. Also shown are a number of contours of constant cost.

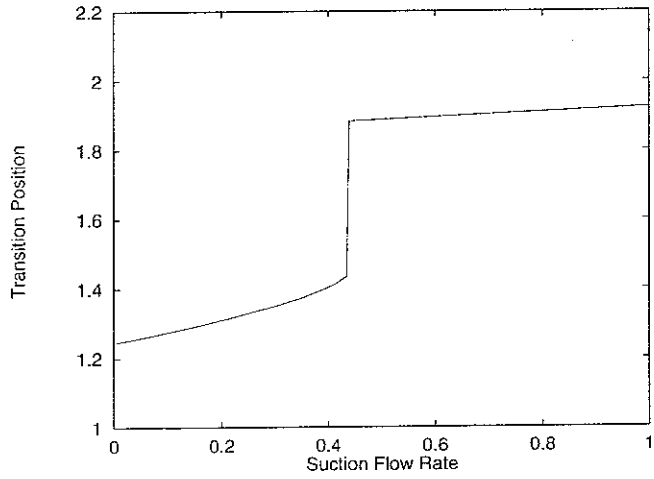

Figure 11: Transition position x_T against the suction flow rate on panel 1 (C_qx10^4) with $C_q = 2\text{x}10^{-4}$ on panel 2.

suction panel, but essentially the same effect would be generated by a similar small change in the suction rate of the second panel. Also, it is clear from figure 12 that discontinuous behaviour would occur with a smaller value of N_T (3.5 or less) and a single suction panel upstream of the hump.

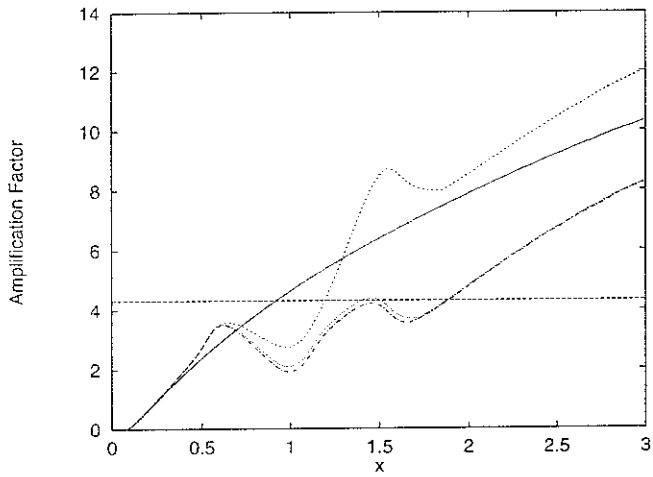

Figure 12: Amplification factor $N(x)$ for a flat plate with nosuction (solid line), a hump with no suction (short dashes), and a hump with two panels and $C_{q1} = 4\text{x}10^{-5}$ and $C_{q2} = 2\text{x}10^{-4}$ (dots), and $C_{q1} = 5\text{x}10^{-5}$ and $C_{q2} = 2\text{x}10^{-4}$ (dot-dash). These lines have predicted transition position of $x_T = 0.92$, 1.20, 1.40 and 1.89 in turn. The dashed line shows the critical value of $n = 4.3$.

So far we have concentrated on the discontinuity on the left of figure 10. However, the contours for $x_T = 1.5$ and 1.6 are virtually the same, and, e.g. when $C_q = 2\text{x}10^{-4}$ on the first panel, x_T jumps from approximately 1.53 to 1.66 when $C_q \approx 1.37\text{x}10^{-4}$. In fact for this configuration there is a band of values of x_T around 1.6 which cannot be accessed with any combination of suction flow rates. A plot of x_T against the suction flow rate on panel two with the rate on panel one fixed with $C_q > 10^{-4}$, would show a discontinuity similar to that seen in figure 11, although with a smaller jump.

For the case with a hump it is clear that the transition position cannot be specified at all positions between the natural transition position with zero suction and the maximum transition position for the given configuration, as a solution may not exist, or may not be achievable with the current algorithm even if it does exist. However, discontinuities can also be found in the simpler flat plate case. For example, for the two panel configuration considered in this section there must be a discontinuity in the surface. The natural transition position of $x_T = 0.92$ lies at the end of the first panel, and if there is no suction of the first panel, then the suction on the second panel will not affect the predicted value of x_T. However, if the second panel has sufficient suction so that N drops well below the critical value of 4.3 in the region of the second panel will a local maximum of N downstream of the first panel, then as the suction on the first panel is increased from zero, the magnitude of the maximum will decrease until it drops below the critical value, when there will be an accompanying jump downstream in the transition position. A contour plot similar to figure 10 was produced, and showed the expected discontinuity in x_T for higher values of C_q on the second panel, but not for the lower values where the suction was not strong enough to produce the required drop in $N(x)$. Hence, although there is a discontinuity in

the surface, there are no regions, i.e. values of x_d between 0.92 and the maximum, which are not achievable. Also, for all values of x_d the optimum value of the cost was sufficiently far away from the discontinuity for the algorithm to converge to the optimum without difficulties.

4. Discussion

The results presented above are for a flat plate with or without an imposed pressure gradient from the external flow, as generic rather than specific examples of suction optimisation problems. Some calculations have also been performed for a NACA 1412 aerofoil, with generally similar results. There is no difficulty in performing such a calculation using the methods outlined above, as they require only the values for $u_{_e}(x)$ behind the stagnation point on the leading edge from potential flow past the body. The calculation was terminated at 50% of chord, as this is before the separation point which occurs in laminar flow, with the inevitable problems for the boundary layer flow calculation. Sample solutions can be found in [8].

It has been shown above that provided that the problem is well specified, the method used quickly converges to a solution. By implication, this has been assumed to be the optimum solution, although except in the two panel case in which the complete solution surface can be mapped, this has not been formally proved. However, we note that if we start from a different point with nonzero initial suction velocities, the final solution produced is the same as that given above. The question of possible local versus global optima should not be ignored in a study of this kind, and it has been found that in at least one case, the flat plate with six panels and $x_d = 2.3$, there is no single optimum solution within the tolerance of the basic solution algorithm. Further, for a different problem, with two panels and an imposed pressure gradient, there are regions between the maximum and minimum transition position which are not accessible, and other positions for which a solution exists but to which the algorithm will not converge. When the optimum occurs at a discontinuity in the solution surface, the method is bound to fail as the gradient estimation step involves constructing a local linear model of the relationship between the suction flow rates and the transition position. Of course, any solution scheme that relies on local smoothness of the underlying data will also fail in such a condition.

We note that although the discontinuities encountered above were in cases with an imposed inviscid pressure gradient, similar discontinuities can easily be generated in the flat plate case. For example, consider a two panel system with one panel ahead of the natural transition position, and the second a reasonable distance downstream of it. Transition will always be upstream of the second panel unless sufficient suction is applied to the first panel to move the transition point close to the leading edge of the second panel. However, if sufficient suction is placed on the second panel to drop the amplification locally well below the critical value, and then the suction rate is increased on the first panel, the transition will move smoothly along the panel until it approaches the second panel, when there will be a sudden jump in the transition

position, similar to that seen above.

The results presented above used the RLS method for the gradient estimation. The alternative finite difference approach was investigated as well for the six panel flat plate case. A centred difference scheme was used in which a small increment was added and subtracted to each of the suction flow rates in turn, and the resulting changes in the transition position used to calculate the components of the gradient vector $\underline{\theta}_k$. Since this requires 13 function evaluations at each iteration, as opposed to one with the RLS algorithm, it is clear that the finite difference method will be more expensive for $x_d = 1.7$, 2.0 and 2.6, when less than 25 iterations where required for convergence using the RLS algorithm. In fact, it took seven to nine iterations (71 to 117 function evaluations) for convergence with the finite difference method, which was therefore significantly more expensive. Note that using a one sided finite difference method, i.e. only adding or subtracting an increment to each suction flow rate, might be cheaper, but would still be expected to be more expensive than the RLS method. For $x_d = 2.3$ the finite difference approach was better behaved than the RLS method in that the algorithm did not show large jumps away from the optimum. However, with the finite difference scheme, the transition position x_T did not achieve the desired value, but displayed a sawtooth oscillation about $x_T = 2.27$. Such oscillations have been noted before, and in some circumstances can be predicted from the local form of the error surface and constraint in the region of the optimum by treating the algorithm as an iterated mapping [5]. For $x_d = 2.9$, the finite difference approach still produced large oscillations in the calculated transition position and cost, although not as large as those found with the RLS method. Allowing μ to decrease with k again produced an algorithm capable of finding and maintaining the optimum solution, although significantly more effort was required than the 50 function evaluations needed with the RLS method. Hence, provided the algorithm is matched to the problem, the RLS approach is consistently cheaper to implement than the finite difference approach. However we note that it is possible that with certain configurations the RLS method of gradient estimation will not produce convergence of the algorithm, whereas the finite difference method will [17].

It was shown above that in certain cases allowing μ to decrease with k could improve the behaviour of the algorithm. However, there may also be disadvantages in this strategy. In practice it is desirable that the algorithm cope with a change in the freestream velocity, but if μ is too small the approach to the optimum will be at least greatly delayed, although the desired transition position should still be achieved as the error dependent term in (16) is not affected by the value of μ. Two runs with the six panel configuration and $x_d = 2.6$ were performed where the freestream velocity $\tilde{U}_\infty$ was increased from 13.3 ms^{-1} to 20ms^{-1} at $k = 75$ and decreased back to 13.3 ms^{-1} at $k = 225$. With $\mu = 0.5$ the algorithm converged to the new state within 50 iterations when the velocity was increased, and within 25 iterations when it was decreased. In contrast, with $\mu = 0.5$ for $k \leq 10$ and $\mu = 2/(k-6)$ for $k > 10$, the algorithm took approximately 250 iteration to come within 10% of the optimum cost following the decrease in velocity at $k = 225$. However, the desired transition position

was obtained more quickly in the case where μ is decaying (25 iterations versus 50 at the increase in velocity and 15 versus 30 at the decrease). Hence, although allowing μ to decay can have advantages, particularly in extreme cases or where the solution is not well defined, in practice it would be necessary to monitor the flow conditions and increase μ where appropriate.

The constrained optimisation problem used here, i.e. minimise the cost while holding the transition at a specified position, is based on the requirements for a nacelle. This formulation is far from unique, and, if the desired position for transition is near the maximum possible position of transition, this may not be a sensible formulation as the suction required may be unrealistically large (see figure 1), or there may be difficulties in finding and maintaining the solution. Other formulations could be considered. For example, for an aerofoil or wing, a more realistic formulation might be to minimise the total energy consumption of the system as a whole, taking into account such factors as the drag, the pump power for the suction system, and the thrust gained by ejecting the fluid sucked through the system back into the external flow. This of course would generate a much more complex problem, for which a different solution algorithm would be required. However, the type of problems encountered above could still appear for other suction optimisation formulations. For example, a simple alternative formulation to that used here would be to fix the cost of the suction and move the transition point as far downstream as possible, which could be regarded as a simple partial model for a system with minimum power consumption. For the two panel case with a forced nonzero pressure gradient considered in §4 of the results, it is clear from figure 10 that for a range of values of the cost, the solution is the transition position on the right of the discontinuity, and hence that a solution algorithm that cannot cope with nonsmooth data would also fail in this case. The question of different formulations and solution algorithms is currently under consideration.

Acknowledgements

This work was supported in part by British Aerospace and the U.K. Engineering and Physical Sciences Research Council, and by the Computational Engineering and Design Centre at Southampton through the provision of computing facilities used during the latter stages of the work.

References

[1] Gad-el-Hak, M., Flow control. *Applied Mechanics Review*, **42**, 261 (1989).

[2] Joslin, R.D., Aircraft Laminar Flow Control, *Annual Review of Fluid Mechanics*, **30**, 1-29 (1998).

[3] Rioual, J.-L., Nelson, P.A. & Fisher, M.J., Experiments of the active control of boundary layer transition. *AIAA J. Aircraft*, **31**, 14416-1418 (1994).

[4] Nelson, P.A., Wright, M.C.M. & Rioual, J.-L., Automatic control of laminar boundary layer transition. *AIAA J.*, **35**, 85-90 (1997).

[5] Nelson, P.A. and Rioual, J.-L. An algorithm for the automatic control of boundary-layer flow. IVSR technical report No. 233, University of Southampton (1994).

[6] Frost, L., An algorithm for linearly constrained adaptive array processing. *Proceedings of the IEEE* **60**, 926 (1972).

[7] Wright, M.C.M. & Nelson, P.A., Experiments on a four channel system for the optimisation of suction distribution for laminar flow control. Submitted to *AIAA J.* (1998).

[8] Hackenberg, P., *Numerical Optimisation of the Suction Distribution for Laminar Flow Control Aerofoils*, Ph.D. thesis, University of Southampton (1994).

[9] Hackenberg, P., Rioual, J.-L., Tutty, O.R. & Nelson, P.A., The automatic control of boundary layer transition - Experiments and computation. *Applied Scientific Research*, **54**, 293-311 (1995).

[10] Carter, J.E. and Wornom, S.F.: Solutions for incompressible separated boundary layers including viscous-inviscid interaction. *Aerodynamic Analysis Requiring Advanced Computers*. NASA SP-347 (1975) 125

[11] Smith, A.M.O.: Transition, pressure gradient, and stability theory. *Proceedings of the 9th International Congress of Applied Mechanics*, Brussels Vol. 4 (1956)

[12] Van Ingen, J.L.: A suggested semi-empirical method for the calculation of the boundary-layer transition region. *Report UTH-74* Univ. of Delft (1956)

[13] Mack, L.M.: Boundary-layer linear stability theory. *AGARD-Report* **709** (1984) 3.1

[14] Nelson, P.A., Rioual, J.-L. and Fisher, M.J.: Experiments on the active control of boundary-layer transition. *Proceedings of the DGLR-AIAA Conference on Aero-Acoustics*, Aachen, Germany (1992) 56

[15] Wellstead, P.E. and Zarrop, M.B.: *Self-Tuning Systems*. John Wiley, Chichester (1991)

[16] Fortescue, T.R. Kershenbaum, L.S. and Ydstie, B.E., Implementation of self-tuning regulators with variable forgetting factors. *Automatica*, **17**, 831 (1981).

[17] Wright, M.C.M. & Nelson, P.A., Gradient estimation issues for on-line laminar flow control. ISVR Technical Memorandum No. 770, University of Southampton (1995).